Enhancement Fault Ride-Through Capability of DFIG by using Resistive and Inductive SFCLs

Ali Azizpour[1], Mehdi Hosseini[2], Mahmoud Samiei Moghaddam[1]
[1]Department of Electrical Engineering, Damghan Branch, Islamic Azad University, Damghan, Iran
[2]Department of Electrical Engineering, Babol University of Technology, Babol, Iran
Corresponiding author, e-mail: AliAzizpour@ymail.com, Mehdie.hosseini@gmail.com,
Samiei352@yahoo.com

Abstract
The number of wind turbines connected to the grid is steadily increasing in recent years. This situation forced the revision of the electric utilities grid codes requirements, to remain connected during grid faults, i.e., to ride through the faults, especially for those with power electronic converters, such as DFIGs. In fault condition, the voltage at the Point of Common Coupling (PCC) drops immediately and The grid voltage dips imposed at the connection point of the DFIG to the grid induce large voltages in the rotor windings, resulting in high rotor current, which can damage the rotor-side converter and disconnect from grid. In this paper, resistive and inductive superconducting fault current limiter (SFCL) is used to improve the fault ride- through (FRT) of wind turbine generation system (WTGS). The WTGS is considered as a variable-speed system, equipped with a DFIG. The analytical and simulation studies of the resistive SFCL for improving FRT capability are presented and compared with the inductive SFCL.

Keywords: SFCL, FRT, variable speed wind turbine (VSWT), DFIG

1. Introduction

Due to growing environmental concerns and demand for electricity, the capacity of electricity generation from renewable energy generation system (REGS) has increased. The wind farms (WFs) are one of the representative renewable energy sources, which are integrated in power system all around the world [1-3].

The large penetration of wind power to existing power systems, have created new challenges such as follows:
a) Increasing short circuit current and,
b) Fault ride through (FRT) capability of wind farms during fault

Different countries have established new grid codes for integration of wind farms to grid, which WFs requires to remain in operation during fault. Such requirements are known as FRT capability [2-3]. There are three most commonly used wind turbines (WTs) in existing wind power industry as follows [2-4]:
a) Fixed speed wind turbine (FSWT),
b) Variable wind turbine (VSWT) based on double fed induction generator (DFIG)
c) VSWT based on permanent magnet synchronous generator (PMSG)

Since, existing WTs have different structure and technology; they have different response to grid fault and requirements to improve FRT capability.

DFIG based WTs widely used because of notable advantages such as: independent control on active and reactive power, operation over a wide range of rotor speed and high efficiency. Several solutions have been proposed to improve FRT capability of DFIG based WTs during fault. Application of crowbar system is widely used to protect the rotor side converter (RSC) and improve FRT [4-5]. The crowbar system consists of a set of resistors connected to rotor side in order to bypass RSC during fault. Although the crowbar system improve the FRT capability of DFIG based WTs, but it absorbs the large amount of reactive power from grid d, which might lead to decrease grid voltage during fault. Many authors have been proposed the application of STATCOM to improve FRT capability of DFIG by reactive power compensation [6-7]. Application of STATACOM is able only to improve voltage recovery after fault clearing. In this paper, the SFCL is proposed to improve FRT capability of DFIG based on WTs, limit the

rotor and stator fault current, and decrease the voltage sag during fault. Various types of SFCL have been developed, which generally are classified as resistive and inductive SFCL. The analytical and simulation studies of the resistive and inductive SFCL for improving FRT capability are presented and compared together. The simulations are carried out by PSCAD/EMTDC software.

2. Superconducting Fault Current Limiter (SFCL)

Superconducting Fault Current Limiter (SFCL) offers a solution to reduce the short circuit level with many significant advantages such as, lossless operation during normal operation and limiting first peak of fault current within sub cycle. Additionally, they can improve reliability and transient stability of power systems by reducing the fault current. There are various types of SFCLs, which generally are classified as resistive and inductive SFCL [8-11].

2.1. Resistive SFCL

A resistive SFCL has advantages such as simpler structure, smaller size, and lower capital cost than other types of SFCL. During normal operation mode, the superconducting element is in its superconducting state, the impedance and power losses are very low. In the case of a short circuit, the SFCL will produce a certain value of impedance within a few milliseconds due to the loss of superconductivity, and insert it into the line for limiting currents in determined value. Many SFCL models have been proposed in order to model the transient behavior of the resistive SFCL during fault. In this paper, a resistive model SFCL is developed in electromagnetic transient program (PSCAD/EMTDC) based on [9-10]. Equation (1) and (2) describe the behavior of resistive SFCL during and after fault. The Eq. 2 describes the resistance generation curve of the SFCL during fault and the Equation (2) expresses the recovery curve of the SFCL after fault. The recovery curve of the SFCL has been modeled with two slopes as reported in [9-10].

$$R_{sc}(t) = R_n \left(1 - \exp\left(-\frac{t - t_0}{T_F} \right) \right) \qquad t_f < t < t_1 \tag{1}$$

$$R_{sc}(t) = \begin{cases} a_1(t - t_1) + b_1 & t_1 < t < t_2 \\ a_2(t - t_2) + b_2 & t > t_2 \end{cases} \tag{2}$$

Where R_n, T_F and t_0 represent the convergence resistance, time constant and quench starting time, respectively. a_1, a_2, b_1, b_2 and t_1, t_2 in the Equation (2), represent the recovery slope, the recovery starting resistance and the recovery starting time, respectively. The characteristic of the resistive SFCL used for analysis is shown in Figure 1.
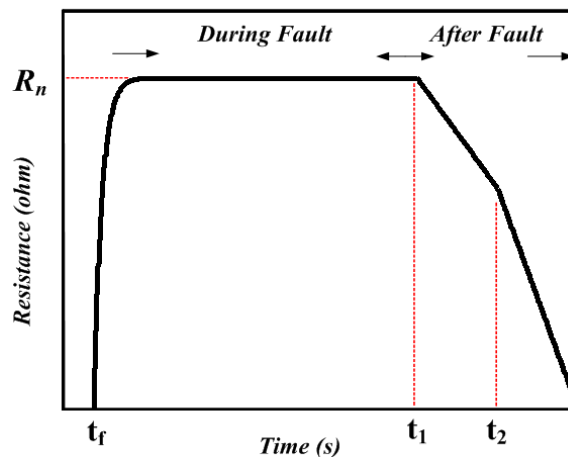

Figure 1. The Characteristic of the Resistive SFCL

2.2. Inductive SFCL

The transformer-type SFCL is shown in Figure 2. This type of FCL basically consists of a transformer in series with the line and a resistive superconducting current limiting device connected to the secondary winding of the series transformer (T) [11-12].

Therefore, the current passing through the SC device is below the critical current and the secondary of the transformer is short-circuited. As a result, the impedance seen by the primary side of the coupling transformer is very low. The resistance of SC devise has to be designed to have larger impedance than magnetizing reactance of transformer.

During fault condition, the SC device generates resistance quickly. As a result, the resistance of SFCL is increased and fault current limited by magnetizing reactance, which is purely inductive. In this case, the impedance of the transformer- type SFCL is expressed as follows:

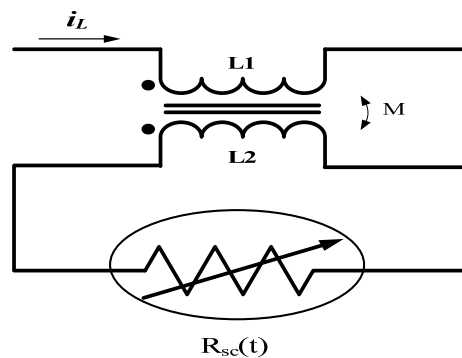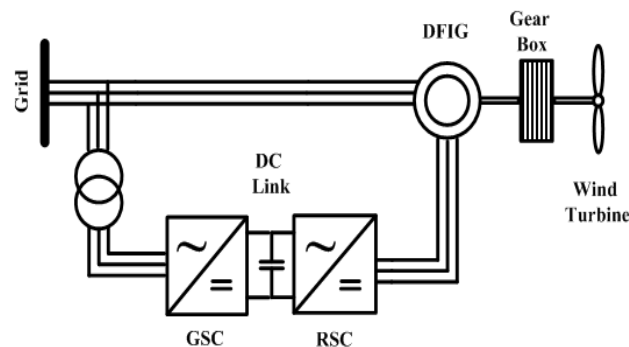$$Z_t = \frac{\omega^2(M^2 - L_1 L_2) + j\omega R_{sc}L_1}{R_{sc} + j\omega L_2} \qquad (3)$$

Figure 2. Transformer-type SFCL

3. Modeling of WECS Based DFIG

The basic configuration of a DFIG is shown in Figure 3. It includes a wounded rotor induction generator (WRIG), which the stator windings of the WRIG are directly connected to the grid. The rotor windings of the WRIG are fed to the same grid through a rotor side converter (RSC) and a grid side converter (GSC) connected by a common DC link capacitor. The rotor of the DFIG is mechanically coupled to the shaft of a DFIG through a mechanical drive train system which consists of a high-speed shaft, a gearbox (GB), and a low-speed shaft. The wind speed model, the model of wind turbine, the mechanical model of the drive-train and induction generator is described in the following sections.

Figur 3. Schematic Diagram of Typical DFIG

3.1. DFIG MODEL

In the synchronous reference frame fixed to the stator flux, the stator and rotor voltages and fluxes can be described as follows:

$$V_s = R_s I_s + L_s \frac{\partial I_s}{\partial t} + L_m \frac{\partial I_r}{\partial t} + j\,\omega_b \Psi_s \tag{1}$$

$$V_r = R_r I_r + L_r \frac{\partial I_r}{\partial t} + L_m \frac{\partial I_s}{\partial t} + j\,\omega_s \Psi_r \tag{2}$$

$$\Psi_s = L_s I_s + L_m I_r \;,\; \Psi_r = L_r I_r + L_m I_s \tag{3}$$

Where, I_s and I_r are the stator and rotor currents, L_s, L_r and L_m are the stator, rotor and magnetizing inductances, respectively, R_s and R_r are the stator and rotor resistances, and ω_b and ω_{slip} are the stator and slip angular frequencies, respectively. From the mathematical model of DFIG [13], the active power and reactive power generated are:

$$P_s = \frac{3}{2} V_s \frac{L_m}{L_s} I_{rq} \tag{4}$$

$$Q_s = \frac{3}{2} \left(\frac{V_s^2}{\omega_s L_s} - \frac{V_s L_m I_{rd}}{L_s} \right) \tag{5}$$

3.2. Wind Speed Model

As shown in Figure 4, wind speed is modeled as the sum of following component: Base wind speed, Gust wind speed, Ramp wind speed and Noise wind speed [14].

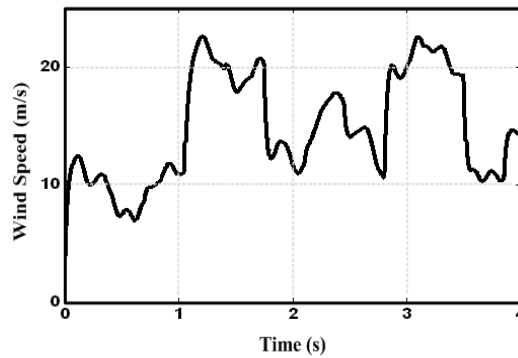The Steady wind speed to the turbine [m/s] is 15m/s.

Figure 4. Wind Speed Model

3.3. Shaft Model/Drive Train System

In order to study the FRT capability of DFIG two mass model systems is used for the shaft system and mechanical dynamics as shown in Figure 5. Two-mass model is defined by [14-15] as follows:

$$\frac{\partial \theta_s}{\partial t} = \omega_s - \omega_g \tag{4}$$

$$T_t = J_t \frac{\partial \omega_s}{\partial t} - K_s \theta_s \tag{5}$$

$$T_e = J_g \frac{\partial \omega_g}{\partial t} - K_s \theta_s \tag{6}$$

Where T_t is the mechanical torque referred to the generator side, T_e is is the electromagnetic torque, J_t is the equivalent turbine-blade inertia referred to the generator side, J_g is the generator inertia, ω_t is the turbine's rotational speed, ω_g is the generator's rotational speed, Ks is the shaft stiffness and θ_s is the angular displacement between the ends of the shaft.
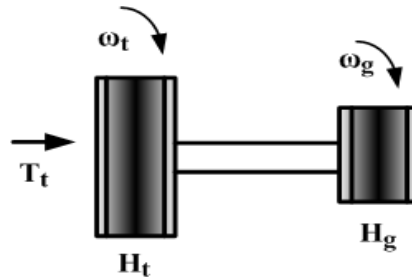

Figure 5. Two Mass Model of Wind Turbine Train

3.4. Wind Turbine Model

The mechanical power generated by wind turbine follows the equation below [14-15]:

$$P_{wt} = \frac{\rho}{2} A_{wt} C_p(\lambda, \theta) v_w^3 \tag{7}$$

Therefore, the mechanical power extracted from the wind (P_{wt}) depends on the air density (ρ), (v_w) is the wind speed, (C_P) is the performance coefficient or power coefficient, λ is the tip speed ration, (A_{wt}) = πR^2 is the area covered by the wind turbine rotor, R is the radius of the tip speed ration and (λ) is defined, as follows:

$$\lambda = \frac{R\,\omega_r}{v_w} \tag{8}$$

The relation between Cp and λ for different pitch angles of β is shown in Figure 6.
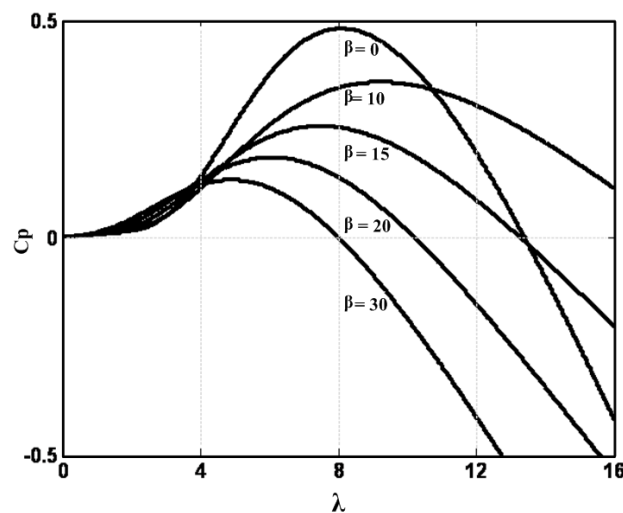

Figure 6. C_P- λ Curves for Different Pitch Angles

4. Simulation Results

A single line diagram of the simulated power system with FCL is shown in Figure 7. The parameters of this system are listed in appendix A. A three phase short circuit fault is simulated on the middle of line 2 (L2), which starts at t=10s. After 0.3 s, the circuit breaker isolated the faulted line. The simulations have been carried out in three states as follow:

a) State 1: Without using FCL (No_FCL)
b) State 2: With resistive SFCL and (R_Type)
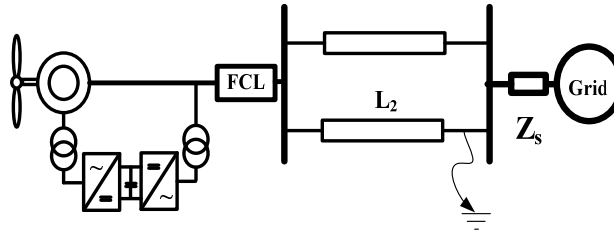c) State 3: With inductive SFCL (L_Type)

Figure 7. Simulated Power System

Figure 8 shows the PCC voltage in three states during fault. It can be observed that not using STATCOM and FCL will lead to the PCC voltage decreases to zero approximately, but can be restored to the normal level. By using resistive and inductive SFCL the PCC voltage not only decreases the voltage sag to 0.7pu and 0.5pu respectively, but also the voltage at PCC can be restored quickly after the fault comparing without FCL.
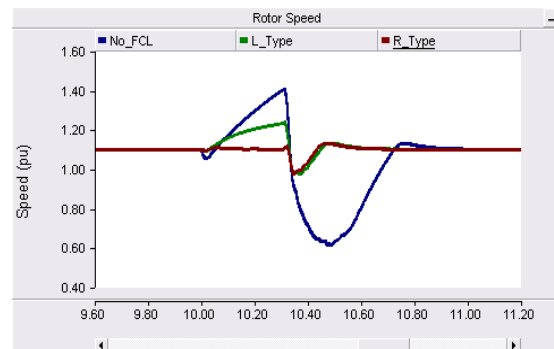
Figure 8. PCC Voltage during Fault in Three States

Figure 9. Rotor Speed during Fault in Three States

Figure 9 shows the rotor speed of the induction generator during fault. As shown in Figure 9, the generator rotor speed swings are reduced in state 2 effectively. These results show that the resistive SFCL can provide an effective damping to the post-fault oscillations comparing states 2 and 3.

Figure 10 and Figure 11 show the total active power generated by the IG and the total reactive power exchange between the IG and the grid, respectively. During the fault the active power generated by the IG is reduced to zero. By using the resistive and inductive SFCL active power generated can be restored quickly after the fault comparing without FCL, which helps to avoid other problems such as voltage collapse and recovery process.
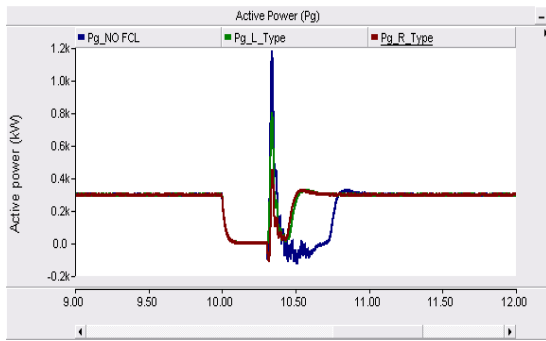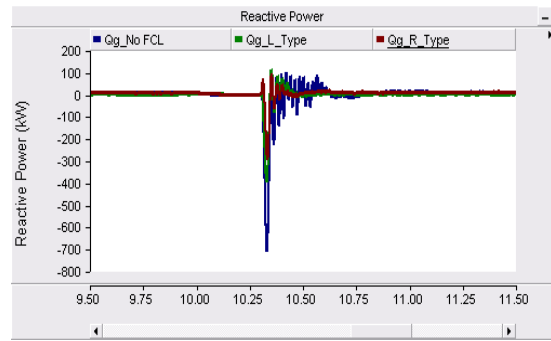
Figure 10. Active Power during Fault in Three States

Figure 11. Reactive Power during Fault in Three States

Figure 12, Figure 13 and Figure 14 show the rotor current IG for three states, respectively. In both figures (Figure 13 and Figure 14), the amplitude of rotor currents is reduced. However, the rotor current transients are significantly reduced in fault instant and after fault clearing in states 2 and 3.
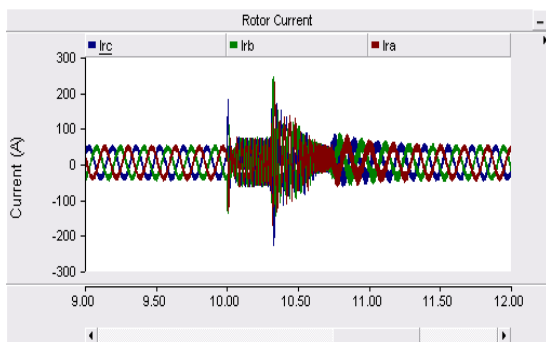

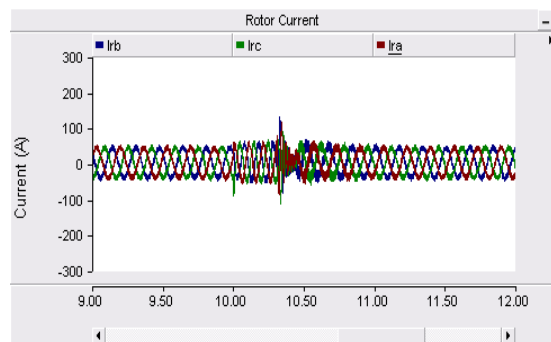Figure 12. Rotor Current during Fault without using any FCL

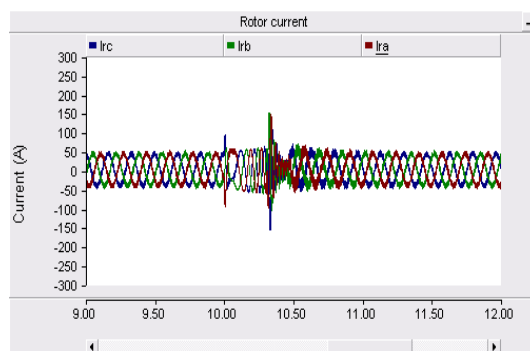Figure 13. Rotor Current during Fault with using Resistive SFCL

Figure 14. Rotor Current during Fault with using Inductive SFCL

5.   Conclusion

In this paper, the application of the resistive and inductive SFCL has been proposed for improving the FRT capability of DFIG and limiting the fault current. The simulation results show that the resistive and inductive SFCL not only limits the fault current but also suppresses the

voltage drop and improves generator stability. Also, the oscillation of active and reactive powers, stator and rotor currents are reduced effectively during fault.

References

[1] JF Manwell, JG McGowan, AL Rogers, Wind energy explained, John Wiley. 2002.

[2] Z Chen, JM Guerrero, F Blaabjerg. A review of the state of the art of power electronics for wind turbines. *IEEE Trans. Power Electron.,* 2009; 24(8): 1859–1875.

[3] JF Conroy, R Watson. Low-voltage ride-through of a full converter wind turbine with permanent magnet generator. *IET Renewable Power Generation*. 2007; 1(3): 182-189.

[4] AH Kasem, EF El-Saadany, HH El-Tamaly. An improve d fault-ride through strategy for doubly fed induction generator based wind turbines. *IET RPG.* 2008; 2(4): 201–214.

[5] F Mei, B Pal. Modal analysis of grid-connected doubly fed induction generators. *IEEE Trans Energy Convers*. 2007; 22(3): 728–36.

[6] SM Muyeen, MA Mannan, MH Ali, R Takahashi, T Murata, J Tamura. Stabilization of wind turbine generator system by STATCOM. *IEEJ Trans. Power Energy*. 2006; 126(10).

[7] M Aten, J Martinez, PJ Cartwright. Fault recovery of a wind farm with fixed speed induction generators using a STATCOM. *Wind Eng*. 29(4): 365–375.

[8] Hector G Sarmiento, R Pampin. *An Example in Controlling Short Circuit Levels in Large Metropolitan Area*. Power Engineering Society General Meeting, IEEE. 2003; 2.

[9] HR Kim, HS Choi, HR Lim, IS Kim, OB Hyun. Resistance of superconducting fault current limiters based on YBa2Cu3O7 thin films after quench completion. *Phys. C, Supercond.,* 2002; 372–376: 1606–1609.

[10] HR Kim, SW Yim, OB Hyun et al. *Analysis o n r ecovery characteristics of superconducting fault current limiters*. Proc. M T-20 Conf. Magn. Technol., Philadelphia, PA. 2007.

[11] H Yamaguchi, T. Kataoka. Effect of magnetic saturation on the current limiting characteristics of transformer type superconducting fault current limiter. *IEEE Trans. Applied Superconductivity*. 2006; 16: 691–694.

[12] T Kataokaand, H Yamaguchi. Comparativestudy of transformer-type superconducting fault current limiters considering magnetic saturation of iron core. *IEEE Trans. Magnetics*. 2006; 42: 3386–3388.

[13] HS Ko, GG Yoon, WP Hong. Active use DFIG-based variable- speed wind-turbine for voltage control in power system operation. *J. Elect. Eng. Technol.,* 2008; 3(2): 254–262.

[14] D Gautam, V Vittal, T Harbour. Impact of increased penetration of DFIG-based wind turbine generators on transient and small signal stability of power systems. *IEEE Trans. Power Syst.,* 2009; 24(3): 1426–1434.

[15] Lin Ye, KP Juengst. Modeling and simulations of resistive type superconducting fault current limiter. *IEEE Trans. Appl. Superconduct.* 2004; 14(2): 839–842.